

Theoretical Studies on Neoclassical Tearing Modes and Their Stabilization

YU Qingquan, GÜNTER Sibylle and LACKNER Karl

Max-Planck-Institut für Plasmaphysik, EURATOM Association, Garching, Germany

(Received: 11 December 2001 / Accepted: 10 April 2002)

Abstract

Numerical simulation results for the nonlinear evolution of neoclassical tearing modes (NTMs) and the stabilization of NTMs by localized RF current drive are presented. It is shown that the saturated island width does not increase linearly with the local bootstrap current density fraction. The NTMs are found to be stabilized by a localized RF current drive, if a sufficiently large RF current is deposited at the rational surface. However, the modulated current drive to deposit the RF current at the o-point of the island has approximately the same stabilizing effect as a continuous RF current drive.

Keywords:

neoclassical tearing mode, magnetic island, nonlinear growth, RF current, modulated current drive, stabilization

1. Introduction

It is well known that classical tearing mode instability is driven by a positive Δ' , the tearing mode index determined by the plasma current density profile and the mode numbers [1]. For a high temperature tokamak plasma, the perturbed bootstrap current usually plays an important role in the nonlinear growth of the tearing modes [2,3]. The inclusion of the perturbed bootstrap current leads to the so called neoclassical tearing mode (NTM). If the fraction of the bootstrap current density is sufficiently large, the saturated magnetic island width is determined by perturbed bootstrap current and Δ' . NTMs have been found to be the most severe limitation of the achievable plasma pressure in tokamaks [4-8].

The driving mechanism of a NTM can be easily understood for a sufficiently large magnetic island. Due to the large ratio between the parallel and the perpendicular transport coefficients the plasma pressure profile is flattened inside the island, and the bootstrap current disappears there. This corresponds to a

perturbation of the equilibrium current density profile. The perturbed current density takes the negative value of the original local equilibrium bootstrap current density at the island's o-point and decays away from the island. This perturbed current is destabilizing for positive magnetic shear, similar to the usual island with an additional noninductive current drive near its o-point in the direction opposite to the equilibrium plasma current.

In recent years both experimental and theoretical efforts have been devoted to NTMs. In the present paper numerical modelling results on two aspects of NTMs, their nonlinear growth and saturation and their stabilization by localized RF current drive, are presented. Two dimensional transport is included in the calculations which is essential for modelling NTMs. It will be shown that the saturated island width is not proportional to the local bootstrap current density fraction for a sufficiently large bootstrap current fraction. NTMs are found to be stabilized by localized

Corresponding author's e-mail: qiy@ipp.mpg.de

RF current drive with an accurate RF wave deposition. However, a modulated current drive to deposit the RF current at the island's o-point has approximately the same stabilizing effect as a continuous RF current drive.

2. Nonlinear evolution of NTMs

The equations describing the NTMs are Ohm's law, the equation of motion, and the pressure evolution equation,

$$\frac{\partial \Psi}{\partial t} + \mathbf{B} \cdot \nabla \phi = E - \eta(j - j_b), \quad (1)$$

$$\rho \left(\frac{\partial}{\partial t} + \mathbf{v} \cdot \nabla \right) \nabla^2 \phi = \mathbf{B} \cdot \nabla j + \rho \mu \nabla^4 \phi, \quad (2)$$

$$\frac{3}{2} \left(\frac{\partial}{\partial t} + \mathbf{v} \cdot \nabla \right) p = \nabla \cdot (\chi_{\parallel} \nabla_{\parallel} p) + \nabla \cdot (\chi_{\perp} \nabla_{\perp} p) + Q, \quad (3)$$

where $\mathbf{B} = B_0 \mathbf{e}_t + \nabla \Psi \times \mathbf{e}_t$ and $\mathbf{v} = -\nabla \phi \times \mathbf{e}_t$ are the magnetic field and velocity, and Ψ and ϕ the magnetic flux function and the stream function, respectively. j is the current density along the \mathbf{e}_t (toroidal) direction, $j_b = -g(\sqrt{\epsilon/B_p}) dp/dr$ the bootstrap current density. g is a function of the minor radius r depending on the collisionality, $\epsilon = r/R$ the inverse aspect ratio, B_p the poloidal field, ρ the mass density, μ the viscosity, p the pressure, Q the heating power, E the equilibrium electric field, and χ the transport coefficient. The subscripts \parallel and \perp denote the parallel and perpendicular components, respectively.

Equations (1)–(3) agree with the reduced MHD equations if the bootstrap current and the parallel and perpendicular transport terms are neglected. The equilibrium toroidal magnetic field is approximated to be a constant, and the toroidal mode coupling is neglected. The bootstrap current is the only toroidal effect included. Since the difference between the particle and the heat transport is not distinguished, eqs. (1)–(3) are valid only for large islands.

According to previous theories [9,10], the following form for χ_{\parallel} is utilized,

$$\chi_{\parallel} = \chi_{\parallel c} \left[1 + \left(3.16 \frac{v_{Te} k_b}{v_e} \right)^2 \right]^{-1/2} \quad (4)$$

where $\chi_{\parallel c} = 3.16 v_{Te}^2 / v_e$ is the classical parallel electron thermal transport coefficient and $k_b = \mathbf{B}_0 \cdot \mathbf{k} / B$ is the parallel wave vector, $v_{Te} = (T_e / m_e)^{1/2}$ is the electron thermal velocity and v_e is the electron collision frequency. In the

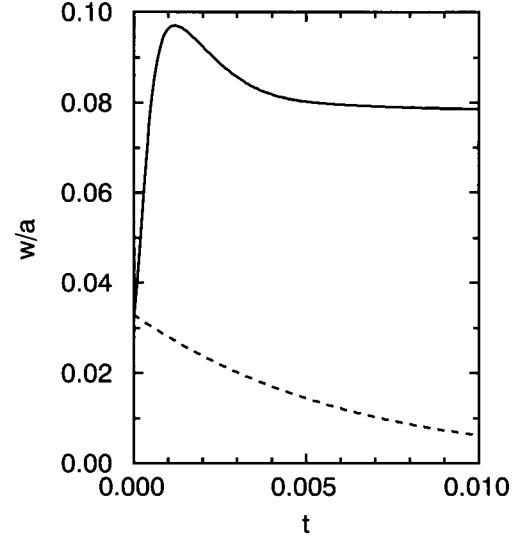


Fig. 1 The normalized 4/3 island width versus normalized time for a local bootstrap current density fraction of 0.22 (solid curve) and 0.038 (dotted curve).

limit $v_e \gg v_{Te} k_b$, Eq. (4) reduces to $\chi_{\parallel} = \chi_{\parallel c}$. In the opposite limit $v_e \ll v_{Te} k_b$, $\chi_{\parallel} = v_{Te} / k_b$ [9]. The χ_{\parallel} given by eq. (4) takes its maximal value at the rational surface and decreases away from it.

The nonlinear time evolution of an $m/n=4/3$ magnetic island width (normalized to the minor radius a) is shown in Fig. 1, where the solid (dotted) curve is obtained with a local bootstrap current density fraction 0.22 (0.038) at the rational surface. The time t is normalized to the resistive time $\tau_R = a^2 \mu_0 / \eta$. $\chi_{\parallel c} = 8.5 \times 10^9 a^2 / \tau_R$, $\chi_{\perp} = 2.4 a^2 / \tau_R$, and $S = \tau_R / \tau_A = 2 \times 10^6$ are taken, where τ_A is the Alfvén time. It is seen that the 4/3 mode is stable for a low bootstrap current density fraction but grows and saturates for a higher one.

In Fig. 2 the saturated $m/n=4/3$ island width is shown as a function of the local bootstrap current density fraction at the rational surface. The saturated island width increases strongly for lower local bootstrap current density fraction but slower for a larger one. Such a behavior suggests that, in addition to the $m/n=4/3$ helical bootstrap current perturbation, additional nonlinear effects are also involved in the mode saturation mechanism.

In Fig. 3 the local current density profile is shown. The solid curve shows the original equilibrium current density profile, and the dotted curve is the $m/n=0/0$ current density profile at island's saturation, corresponding to the solid curve of Fig. 1 at $t=0.01 \tau_R$.

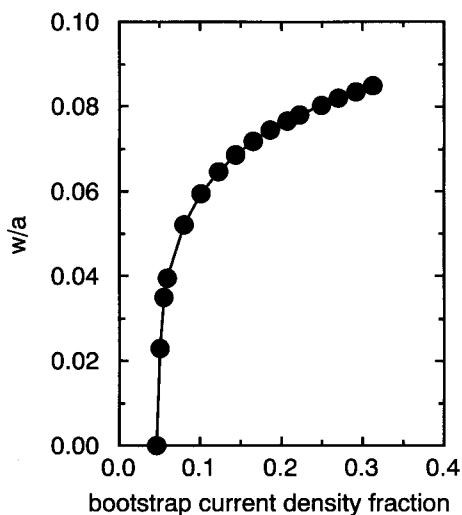


Fig. 2 The saturated 4/3 island width versus the local bootstrap current density fraction.

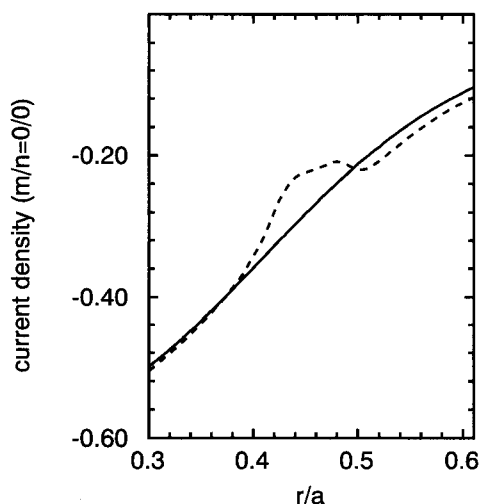


Fig. 3 The original equilibrium current density profile (solid curve) and the $m/n=0/0$ current density profile at island's saturation (dotted curve), corresponding to Fig. 1 at $t=0.01$.

The equilibrium plasma current is in the negative e_t direction in the opposite direction to the toroidal magnetic field, and therefore it is negative. The equilibrium rational surface is at $r_s=0.46a$. The local $m/n=0/0$ current density and the current density gradient is reduced around the rational surface due to zero bootstrap current inside the island. The change of the local current density profile leads to a corresponding change of the local safety factor q profile. The rational

surface shifts inwards towards the magnetic axis, and the local magnetic shear is increased. Such a change in the $m/n=0/0$ current density profile and the q profile is found to have a more significant effect on the saturated island width in a small magnetic shear region [11].

It is therefore clear that, the disappearance of the bootstrap current inside the island leads to both a helical component and a $m/n=0/0$ component current density perturbation. The helical component is destabilizing, while the $m/n=0/0$ component, leading to a new equilibrium current profile, is stabilizing. This explains the slower than linear increase of the saturated island width in the large bootstrap current density fraction region, as shown in Fig. 2.

3. Stabilizing NTMs by localized RF current drive

Because NTMs limit the confinement of tokamak plasmas, one should try to stabilize these modes. A straightforward stabilization method is to use localized RF current drive to fill the current hole caused by the disappearance of the bootstrap current inside the island. It has recently been shown on ASDEX Upgrade that localized ECCD can reduce the mode amplitude to zero [12,13].

To model the effect of RF current on NTMs, Ohm's law is modified to the form

$$\frac{\partial \psi}{\partial t} + \mathbf{v} \cdot \nabla \psi = E - \eta(j - j_b - j_d), \quad (5)$$

where j_d is the RF drive current source term.

The RF driven current is caused by the asymmetric heating of electrons in the velocity space. The resulting fast electrons have a much longer slowing down time than the thermal ones. The corresponding time scale is usually in the range 0.1–1ms for ECCD, and even longer for LHCD for high temperature tokamak plasmas [10,14]. The fast electrons will diffuse in space while they slow down, and therefore the driven current profile depends on both the wave deposition profile and the fast electron transport. In the presence of a magnetic island both the parallel and the perpendicular transport affect the profile of the driven current. To take into account these effects, the fast electron density is described by the two dimensional transport equation [10]

$$\frac{\partial n_f}{\partial t} = \nabla \cdot (\chi_{\parallel f} \nabla_{\parallel} n_f) + \nabla \cdot (\chi_{\perp f} \nabla_{\perp} n_f) + \nu_f (n_{fs} - n_f), \quad (6)$$

where n_f is the fast electron density, $\chi_{\parallel f}$ and $\chi_{\perp f}$ are the

parallel and perpendicular transport coefficients of the fast electrons, and v_f^{-1} is the slowing down time of the fast electrons. n_{fs} is the fast electron source due to the RF waves given by [10,14]

$$n_{fs} = n_{fs0} \exp \left[-2 \left(\frac{r - r_{ds}}{w_{ds}} \right)^2 \right] \Pi(h_0, \Delta h), \quad (7)$$

where n_{fs0} is the magnitude of the source, w_{ds} is the radial half-width of the fast electron density profile, and r_{ds} is the deposition radius where n_{fs} has its maximal value.

The square box function $\Pi(h_0, \Delta h)$ in eq. (7) takes into account the effect of island rotation [10,14]. We assume that the island does not rotate, and its o-point and x-point are at the helical angle $h = m\theta + n\phi = 0$ and $\pm\pi$ respectively, while the instantaneous wave deposition width along the helical angle, $\Delta h = m\Delta\theta + n\Delta\phi$, rotates with respect to the island at an angular frequency ω . $\Pi(h_0, \Delta h)$ is defined as $\Pi(h_0, \Delta h) = 1$ for $|h - h_0| < \Delta h$ and $h_{on} < h_0 < h_{off}$, and $\Pi(h_0, \Delta h) = 0$ elsewhere, where, $h_0 = \omega t$ and h_{on} (h_{off}) is the helical angle at which the RF wave is turned on (off). When $h_{on} = -\pi/2$ and $h_{off} = \pi/2$, the wave deposition and the resulting fast electron source are located around the o-point of the island, and we will call this case the modulated current drive (MCD). When $h_{on} = -\pi$ and $h_{off} = \pi$, the fast electron source rotates along all the helical angle corresponding to a continuous RF current drive in time, and we will call this case the non-modulated current drive (NMCD).

Since the driven current is caused by the fast electrons, we assume the driven current density j_d to be proportional to the fast electron density, $j_d = c_f n_f$. The total driven current I_d is obtained by integrating j_d over the plasma cross section. The constants c_f and n_{fs0} in eq. (7) can be determined from I_d . Similarly, the source current, I_{ds} , can be obtained by assuming the source current density $j_{ds} = c_f n_{fs}$, and integrating j_{ds} over the plasma cross section. The half width w_{ds} and the total RF source current I_{ds} can be obtained from a ray-tracing and Fokker-Planck code [14].

The growth and saturation of an $m/n=3/2$ magnetic island driven by a perturbed bootstrap current is shown by the solid curve in Fig. 4. The equilibrium bootstrap current density fraction is 0.14 at the $q=3/2$ surface located at $r=0.58a$. After the RF current is turned on at $t=0.01\tau_R$, the time evolution of the island width is shown by the dotted curve for the NMCD, where $I_{ds}/I_p=0.021$, $w_{ds}/a=0.04$, $\chi_{\perp}=23a^2/\tau_R$, $\chi_{\perp f}=3.0a^2/\tau_R$, $\Delta h=0.482$, $\omega=5 \times 10^4/\tau_R$, $v_f=4 \times 10^3/\tau_R$, and $\chi_{\parallel f}=\chi_{\parallel}$ with

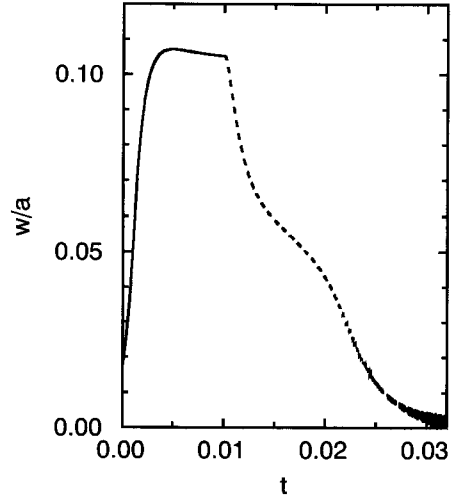


Fig. 4 The normalized 3/2 island width versus the normalized time before (solid curve) and after (dotted curve) RF current is turned on.

$\chi_{\parallel c} = 2.1 \times 10^9 a^2 / \tau_R$ are taken. The minor radius of the RF current peak, r_{ds} , is chosen to be at the $q=3/2$ rational surface r_s . It is seen that a sufficient large RF current can stabilize the NTM. The MCD can also stabilize the 3/2 mode with the same parameters as given above.

In Fig. 5 the time evolution of the island width is shown after the RF current is turned on at $t=0.01\tau_R$, with $I_{ds}/I_p=0.01$ for both the MCD (solid curve) and the NMCD (dotted curve), and all the other parameters being the same as in Fig. 4. It is seen that the island width is reduced to approximately the same level for the MCD or the NMCD case. The reason for such results is that, although the RF source current is modulated for the MCD to deposit the RF current at the o-point of the island to have a larger $m/n=3/2$ component, for the NMCD the $m/n=3/2$ component of j_d is also formed due to the geometry and the transport, since the fast electrons generated near the x-point of the island diffuse along the field lines to a larger area around the island, and the driven current density there is therefore small. While the fast electrons generated around the o-point of the island can only diffuse away by perpendicular transport which is much slower than the parallel transport. Therefore, for NMCD the driven current density is also larger at the o-point of the island than elsewhere, and the $m/n=3/2$ component j_d is close to that of MCD. The slightly larger stabilizing effect for the NMCD is due to a larger change of the local $m/n=0/0$ component current density gradient, since $I_d=I_{ds}$ for the

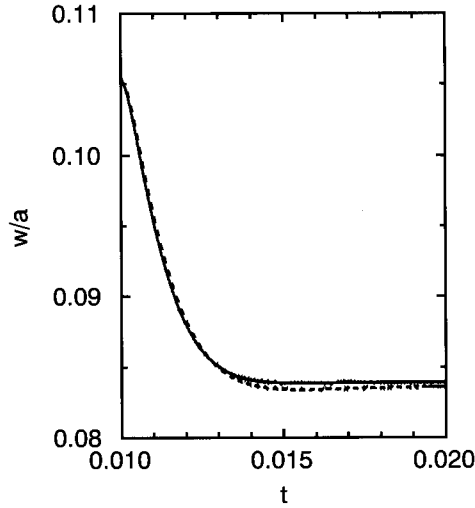


Fig. 5 The normalized island width versus the normalized time for MCD (solid curve) and NMCD (dotted curve).

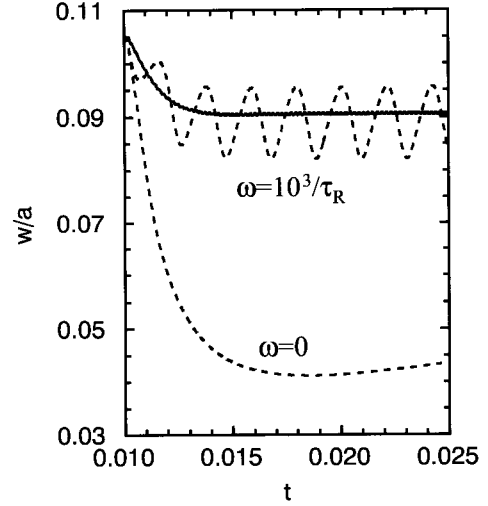


Fig. 6 The normalized island width versus the normalized time for $\omega=10^4/\tau_R$ (solid curve), $10^3/\tau_R$ (dotted curve), and 0 (dashed) after RF current is on.

NMCD and $I_d=0.5I_{ds}$ for the MCD.

Usually a magnetic island rotates with respect to the laboratory frame with $\omega/v_f \gg 1$. However, when $\omega/v_f < 1$, I_d will reach I_{ds} in one cycle, and a larger stabilizing effect is achieved as seen from Fig. 6, where the time evolution of the magnetic island width is shown for $\omega=10^4/\tau_R$ (solid), $10^3/\tau_R$ (dotted) and 0 (dashed), respectively, for $I_{ds}/I_p=0.007$ and NMCD. All other input parameters are the same as those for Fig. 4. It is seen that, for a larger ω , $\omega=10^4/\tau_R$, the island width decreases to a steady value similar to Fig. 5. When $\omega=5 \times 10^4/\tau_R$, the result is approximately the same as that with $10^4/\tau_R$. For a smaller ω , $\omega=10^3/\tau_R$, the island width oscillates in time because of the rotation of the RF current deposition along the helical angle. The time averaged island width is the same as that with $\omega/v_f \gg 1$, but a minimal value of the island width exists which is helpful for the stabilization, as the perturbed bootstrap current is not able to drive the mode unstable for an island width smaller than the seed island width [8]. For $\omega=0$ the RF current source is always on and localized around the o-point of the island with a deposition width Δh along the helical angle, and $I_d=I_{ds}$ in a time scale v_f^{-1} , which corresponds to a larger $m/n=3/2$ component of j_d and therefore a stronger stabilizing effect.

For $\omega/v_f \gg 1$, no significant effect of Δh on the stabilization has been found for both MCD and NMCD with Δh varying from 0.1 to 1.0, while for $\omega/v_f < 1$, the stabilizing effect is found to be larger for a smaller Δh .

In Fig. 7 the normalized island width is shown as a function of the normalized time for $\Delta h=0.4$ (solid curve) and 0.8 (dotted curve), respectively, where $\omega=0$ and $I_{ds}/I_p=0.014$ are taken, and all the other input parameters are the same as those for Fig. 4. It is seen that the island width decreases as Δh decreases due to a larger helical component of j_d for a smaller Δh .

The major difficulty encountered in the experiments of stabilizing NTMs using localized current drive is to identify the exact location of the rational surface. If r_{ds} is shifted from r_s , the stabilizing effect is weaker as shown in Fig. 8, in which the time evolution of the island width is shown for $dr=(r_{ds}-r_s)/a=0.005$ (solid curve), 0.02 (dotted curve) and -0.015 (dashed curve), respectively, where $I_{ds}/I_p=0.03$ is taken. It is seen that the suppression of the NTM is possible if dr is sufficiently small.

4. Discussion and Summary

In the present paper it is shown that the increase of the saturated island width with the local bootstrap current density fraction is slower than linear because of the change of the $m/n=0/0$ current profile due to the disappearance of the bootstrap current inside the island. For a high bootstrap current density fraction, the saturated island width tends to saturate. The numerical results agree with the experimental observation [7].

The NTMs are found to be stabilized by localized RF current, if the RF wave deposition location is

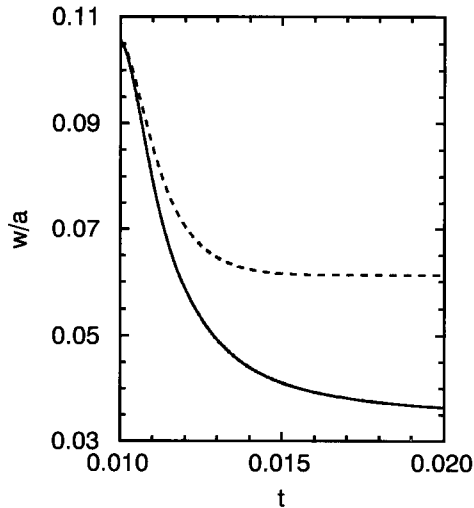


Fig. 7 The normalized island width versus the normalized time for $\Delta h=0.4$ (solid) and 0.8 (dotted).

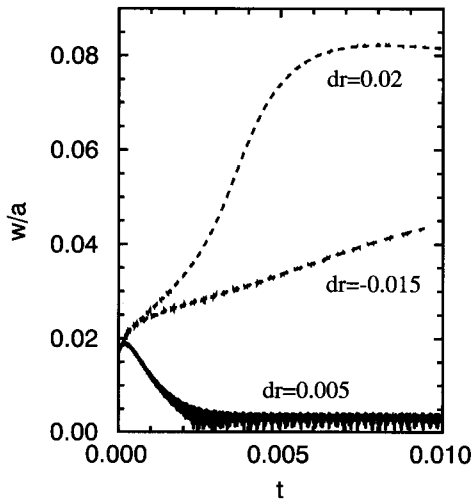


Fig. 8 The normalized island width versus the normalized time for $dr=0.005$ (solid), 0.02 (dotted) and -0.015 (dashed).

sufficiently accurate. However, there is no advantage to modulate the current drive to deposit the RF current at the o-point of the island, since the transport along the magnetic field in the island geometry will lead to a larger RF current density at the o-point than that at the x-point of the island. This agrees with the experimental results that MCD has approximately the same stabilizing effect as a continuous RF current [12]. Our numerical studies also show that, for $\omega/v_T < 1$ the island width oscillates in time due to the relative rotation between the

RF current deposition and the island. In this case if the minimal value of the island width is smaller than the seed island width, the mode will be stabilized [8]. When $\omega/v_T < 1$, a smaller instantaneous wave deposition width Δh along the helical angle leads to a larger stabilizing effect. These results suggest that a slow rotating NTM is more easily to be stabilized by the RF current, especially when Δh is small.

In conclusion, our numerical results indicate that:

- (1) The saturated island width tends to saturate for high bootstrap current density fraction.
- (2) A continuous RF current has about the same stabilizing effect as a modulated one.

Acknowledgment

Q. Yu was partially supported by the Institute of Plasma Physics, Chinese Academy of Science (CAS) and the "one hundred elite" project of CAS during the work presented.

References

- [1] H.P. Furth, J. Killen and M. N. Rosenbluth, *Phys. Fluids A* **6**, 459 (1963).
- [2] National Technical Information Service Document, No. DE86008946 (University of Wisconsin Plasma Report UWPR 85-5 by W.X. Xu and J.D. Callen).
- [3] R. Carrera, R.D. Hazeltine, and M.Kotschenreuther, *Phys. Fluids A* **29**, 899 (1986).
- [4] Z. Chang, J.D. Callen, E.D. Fredrickson *et al.*, *Phys. Rev. Letts.* **74**, 4663 (1995).
- [5] H. Zohm, G. Gantenbein, A. Gude *et al.*, *Nucl. Fusion*, **41**, 197 (2001).
- [6] R.J. La Haye, L.L. Lao, E.J. Strait *et al.*, *Nucl. Fusion* **37**, 397(1997).
- [7] S. Günter, A. Gude, M. Maraschek *et al.*, *Plasma Phys. Control. Fusion* **41**, 767 (1999).
- [8] S. Günter, A. Gude, M. Marschek *et al.*, *Nucl. Fusion* **38**, 1431 (1998).
- [9] Z. Chang and J.D. Callen, *Phys. Fluids B* **4**, 1167 (1992).
- [10] Q. Yu, S. Günter, G. Giruzzi *et al.*, *Phys. Plasmas* **7**, 312 (2000).
- [11] Qingquan Yu and Sibylle Günter, *Plasma Phys. Control. Fusion* **40**, 1989 (1998).
- [12] H. Zohm, G. Gantenbein, G. Giruzzi *et al.*, *Nucl. Fusion* **39**, 577 (1999).
- [13] G. Gantenbein, H. Zohm, G. Giruzzi *et al.*, *Phys. Rev. Letts.* **85**, 1242 (2000).
- [14] G. Giruzzi, M. Zabiego, T.A. Gianakon *et al.*, *Nucl. Fusion* **39**, 107 (1999).